

in which case $\Delta h \cong \pm 0.5$ naut mile in the q th quadrant for low-altitude orbits.

It is interesting to note that when $i_0 = 0$, both B and e become zero, and hence $\Delta h = 0$, which says that, for an equatorial orbit, a "circular" orbit gives the minimum altitude variation. In addition, a polar orbit gives the greatest altitude variation.

References

¹ Struble, R. A. and Campbell, W. F., "Theory of motion of a near earth satellite," ARS J. 31, 154-155 (1961).
² Rider, L., "A class of minimum altitude variation orbits about an oblate earth," Aerospace Corp., El Segundo, Calif., TDR-594 (1560-01) TN-2 (March 1961); also ARS J. 31, 1580-1582 (1961).
³ Anthony, M. L. and Fosdick, G. E., "Satellite motions about an oblate planet," J. Aerospace Sci. 28, 789-802 (1961).
⁴ Kalil, F., "Effect of an oblate rotating atmosphere on the eccentricity, semimajor axis, and period of a close earth satellite," The Martin Co., ER 12552 (April 1962) and ER 12511 (May 1962); also AIAA J. (to be published).
⁵ Sterne, T. E., "Effect of the rotation of a planetary atmosphere upon the orbit of a close satellite," ARS J. 29, 777-782 (1959).
⁶ Brouwer, D. and Hori, G., "Theoretical evaluation of atmosphere drag effects in the motion of an artificial satellite," Astron. J. 66, no. 5, 193-225 (1961).
⁷ Brouwer, D. and Hori, G., "Appendix to theoretical evaluation of atmospheric drag effects in the motion of an artificial satellite," Astron. J. 66, no. 6, 264-265 (1961).
⁸ King-Hele, D. G., "The effect of the earth's oblateness on the orbit of a near satellite," Proc. Roy. Soc. (London) 247A, 49-72 (August 1958).
⁹ King-Hele, D. G., Cook, G. E., and Walker, D. M. C., "Contraction of satellite orbits under the influence of air drag, Part I, with a spherically symmetrical atmosphere," Royal Aircraft Establishment, Farnborough, England, TN G.W. 533 (November 1959).
¹⁰ King-Hele, D. G., Cook, G. E., and Walker, D. M. C., "The contraction of satellite orbits under the influence of air drag, Part II, with oblate atmosphere," Royal Aircraft Establishment, Farnborough, England, TN G.W. 565 (December 1960).

Cryogenic Propellant Stratification Analysis and Test Data Correlation

T. BAILEY,* R. VANDEKOPPEL,† G. SKARTVEDT‡
Martin Company, Denver, Colo.

AND

T. JEFFERSON§
University of Arkansas, Fayetteville, Ark.

Nomenclature

- A_H = tank wall heated area
- A_{HC} = heated area opposite cold layer
- C_p = liquid specific heat
- h = liquid film heat-transfer coefficient
- q = heat-transfer rate through unit area of tank wall
- u = velocity of fluid in boundary layer
- V_H = volume of warm layer
- y = distance in boundary layer measured from wall
- δ = boundary-layer thickness

Received by ARS June 29, 1962; revision received April 17, 1963.

* Design Engineer.
 † Design Specialist. Member AIAA.
 ‡ Unit Head.
 § Head, Mechanical Engineering Department.

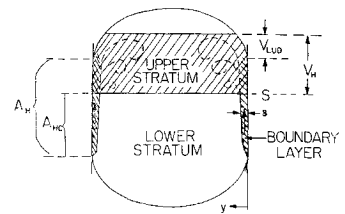


Fig. 1 Analytical model

- θ = temperature excess (actual temperature minus liquid-bulk temperature)
- θ_w = wall temperature minus liquid-bulk temperature
- ρ = liquid density
- H = liquid enthalpy per unit mass
- D = tank diameter

ONE of the primary objectives of a liquid rocket propellant pressurization and feed system is to supply propellant to the engine at the required pressure and flow rate. For a pump-fed engine, sufficient pressure is required to suppress cavitation in the pump. This pressure usually is specified in terms of a minimum net positive suction head (NPSH) value, with NPSH defined as the difference between total pressure and vapor pressure at the pump inlet. The rocket designer must provide the required margin between total pressure and vapor pressure at all times during flight. Design of cryogenic propellant systems in particular requires detailed analysis of transient temperature distributions within the propellant resulting from aeroheating. A variety of test data is available which indicates a strong tendency toward stratification; the upper propellant layers experience a large increase in vapor pressure, and the lower layers show little or none. The upper layers may or may not be saturated, depending on the system operating parameters.

An analytical procedure has been developed to accomplish quantitative analysis of the stratification phenomenon. Development of the analysis proceeds from basic considerations, and no scale-effect factors or other gross empirical coefficients are required. Results of the analysis consist of volume and temperature of the warm upper propellant layer as functions of time. Correlations of predicted results with liquid nitrogen ground-test data and liquid oxygen Titan and Vanguard flight-test data confirm the validity and usefulness of the analytical model.

Analytical Model

The stratification analysis is based on integration of liquid mass flow in the natural convection boundary layer along the heated tank wall. The primary assumptions of the analysis are that 1) the initial temperature of the liquid is uniform, 2) all the heat input to the tank wall appears as sensible heat in the boundary layer, 3) all the flow in this boundary layer goes into a warm upper stratum and remains there, 4) this warm stratum is uniformly mixed, and 5) there is no mixing between the warm stratum and the lower unheated stratum.

Consider the horizontal plane S separating the two strata, as shown in Fig. 1. The growth of the upper stratum results from the flow in the boundary layer that crosses S . This flow is confined to the annular ring in S , of width δ , inside the tank wall. Applying an energy balance to that portion of the boundary layer below S and assuming that the thermal energy stored in the boundary layer is negligible, there results the equation

$$q A_{HC} = \pi D \int_0^\delta \rho [H(y) - H_0] u(y) dy \tag{1}$$

Assuming constant specific heat and density, this can be written as

$$q A_{HC} = C_p \rho \pi D \int_0^\delta \theta(y) u(y) dy \tag{2}$$

The volumetric flow rate through S and hence the rate of increase of the warm stratum volume is given by the equation

$$\dot{V}_H = \pi D \int_0^\delta u(y) dy \quad (3)$$

Multiplying both sides of Eq. (3) by $q A_{HC}$ and dividing by Eq. (2) gives the result

$$\dot{V}_H = \frac{q A_{HC}}{C_p \rho} \left[\int_0^\delta u(y) dy / \int_0^\delta \theta(y) u(y) dy \right] \quad (4)$$

For the propellants, heating rates, and tank sizes encountered in rocket design, $N_{Gr} \gg 10^9$; and the boundary layer is, therefore, turbulent. Measurements of temperature and velocity profiles in turbulent free-convection boundary layers can be correlated with the equations¹

$$u(y) = u_1(y/\delta)^{1/7} [1 - (y/\delta)]^4 \quad (5)$$

and

$$\theta(y) = \theta_w [1 - (y/\delta)^{1/7}] \quad (6)$$

Introducing these into Eq. (4) and performing the necessary integrations leads to the result

$$\dot{V}_H = (q A_{HC} / C_p \rho) (4.0 / \theta_w) \quad (7)$$

Since $q = h \theta_w$, this can be written as

$$\dot{V}_H = (4.0 h A_{HC} / C_p \rho) \quad (8)$$

This equation shows that the volume rate of growth of the upper stratum can be determined if the inside heat-transfer coefficient is known. This coefficient can be determined from the known heat input rate, together with a suitable correlation of heat-transfer coefficient vs heat flux. Although the numerical constant 4.0 just obtained is strictly applicable only for turbulent free-convection boundary layers, this value is not very sensitive to the exact shape of the profiles.

The instantaneous volume flow rate of propellant into the warm layer, as given by Eq. (8), must be integrated with respect to time to determine the progress of stratification over a finite time interval. The temperature of the warm stratum is obtained from an energy balance:

$$\theta_H = \int_0^t q A_H dt / \rho C_p V_H \quad (9)$$

Comparison of Analytical Results with Test Data

The validity of the analytical model is demonstrated by comparison of predicted analytical results with experimental results. Both ground-test and flight-test data are used for the comparison.

The ground tests were performed with liquid nitrogen in a full-scale second-stage Titan oxidizer tank. The tank was equipped with a helium pressurization system that supplied programed tank pressures, a heating chamber to provide programed heating of the barrel portion of the tank wall, and instrumentation to measure nitrogen temperature distribution. The controlled variables in the tests were tank pressure, heating rate, test duration, and quantity of nitrogen in the tank. The tank was not drained during the tests.

Analytical simulations of these test conditions were made on a digital computer. Data input for the computer runs duplicated as closely as possible the geometries, heating rates, pressures, and durations experienced in the tests. The value used for h depended on the heat-transfer mechanism. For free convection, the equation recommended by McAdams²

$$\frac{hL}{K_f} = 0.13 \left[\frac{L^3 \rho_f^2 g \beta_f \Delta T}{\mu_f^2} \left(\frac{C_p \mu}{K} \right)_f \right]^{1/3}$$

was used. For nucleate boiling, h was calculated from the

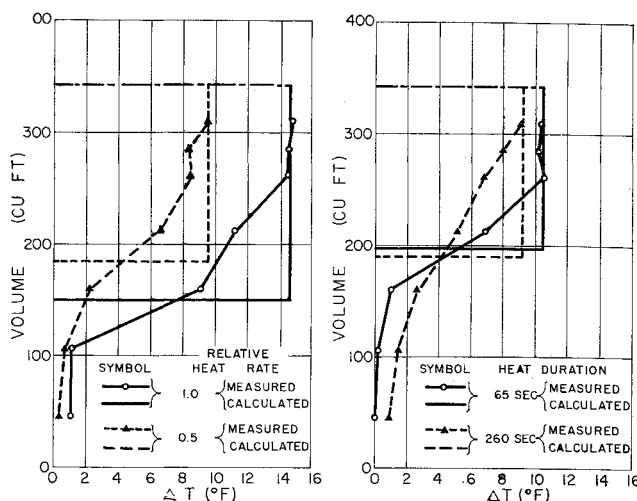


Fig. 2 Effects of heating rate and duration

equations

$$q = C(T_{wall} - T_{sat})^{3.5}$$

and

$$h = \frac{q}{T_{wall} - T_{liq}}$$

The value of C was chosen to give a good fit for data from several sources.

Figure 2 shows the comparison between analytical and measured temperature profiles for four tests with varying conditions of heating rate and duration. The data in each case correspond to the end of the heating period. A ΔT of 17°R corresponds to saturation temperature at the tank pressure of 32 psia. Figure 2 shows that the liquid in the warm layer did not reach saturation temperature in any of the four tests.

Figure 3 shows a similar comparison of analytical results with Vanguard and Titan liquid-oxygen temperature measurements obtained during flight tests. The comparison is based on liquid-oxygen temperature at the pump inlet as a function of time during the period of propellant consumption.

The comparison figures indicate that the maximum measured temperature rise in the warm layer was calculated within roughly $\pm 10\%$ of the measured change for both the ground and flight tests. In addition, effects of variation of controlled variables in the ground tests were predicted correctly. Considerable mixing of the warm and cold layers is evident in contrast to the no-mixing assumption used in the analysis; however, to the designer interested in supplying

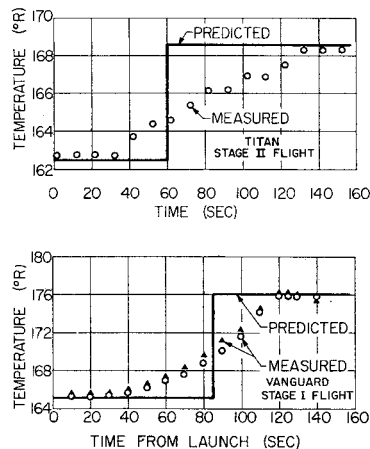


Fig. 3 Liquid-oxygen temperature histories at pump inlet for Titan stage II and Vanguard stage I flights

adequate pump NPSH, the ability to predict maximum temperatures encountered at the pump inlet is of considerable value.

References

- ¹ Eckert, E. R. G. and Jackson, T. W., "Analysis of turbulent free convection boundary layer on a flat plate," NACA Rept. 1015 (July 12, 1950).
- ² McAdams, W. H., *Heat Transmission* (McGraw-Hill Book Co. Inc., New York, 1954), 3rd ed., p. 172.

Validity of Series Expansions of Kepler's Equation

ERWIN W. PAUL*
*Westinghouse Electric Corporation,
Baltimore, Md.*

A solution of the Kepler equation $M = E - e \sin E$ is discussed. In digital computation, very often preference is given to a Taylor expansion progressing in powers of the time. The complex representation of the Kepler equation as an analytical function shows clearly the limited interval of convergence.

THE complete solution of the problem of the motion of a satellite in its elliptical orbit includes the solution of the Kepler equation

$$M = E - e \sin E$$

The mean anomaly, M , is essentially a time measure, and E and e are the eccentric anomaly and the eccentricity, respectively.

The Kepler equation is transcendental in E . Therefore, an analytical presentation of $E = E(M, e)$ can be found only approximately by some series expansion of E . Two expansions are common, namely:

1) The Fourier-Bessel expansion, progressing in multiples of the variable M :

$$E = M + 2 \sum_{p=1}^{\infty} \frac{J_p(pe)}{p} \sin(pM)$$

The Bessel coefficients depend on the fixed value of e . This expansion is valid for $0 \leq e < 1$ for all values of M .

2) The Taylor expansion of E , progressing in powers of the variable e :

$$E = \sum_{p=0}^{\infty} B_p(M) e^p$$

The coefficients depend on the fixed value of M . This expansion is due to Lagrange and converges for $0 \leq e < 0.6627$ for all values of M . The details of such expansions can be found, for example, in Refs. 1 and 2.

In digital computation, very often preference is given to Taylor expansions progressing in powers of the time, or equivalently, in powers of the mean anomaly. Of course, the validity of such an expansion is likewise restricted to the

Received by ARS October 23, 1962; revision received March 29, 1963. This research was sponsored by the U. S. Air Force under Contract AF 49(638)1002 monitored by the Office of Scientific Research of the Office of Aerospace Research. The writer is indebted to George Shapiro, Advisory Mathematician of the Westinghouse Air Arm Division, for his helpful suggestions and criticisms during the preparation of this paper. He also thanks the reviewer for calling Ref. 3 to his attention.

* Fellow Engineer, Computing and Control Systems, Air Arm Division.

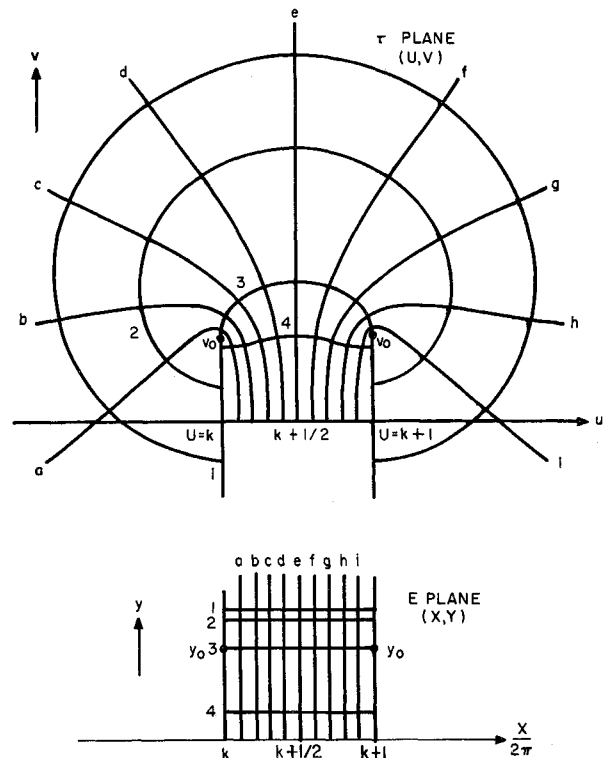


Fig. 1 The conformal mapping of $x = \text{const}$ and $y = \text{const}$

region of convergence which can best be found by means of the theory of analytical functions. It is important to know the radius of convergence, which is equal to the distance from the point about which the expansion is performed to the nearest singularity, which in the complex representation is mapped as a critical point. In the following, the convergence of this type of Taylor expansion of E is discussed, namely:

3) The Taylor expansion of E , progressing in powers of M :

$$E = \sum_{p=0}^{\infty} C_p(e) (M - M_1)^p$$

The coefficients depend on the fixed value of e . In order to simplify the expression for the mean anomaly, M , the convention is made that the satellite passes perigee at time zero. Then the mean anomaly is $M = 2\pi(t/T)$, where T is the period of revolution and t is the time.

Introducing the time ratio $\tau = t/T$ rather than the mean anomaly M , the Kepler equation is written as

$$\tau = (1/2\pi)(E - e \sin E) \tag{1}$$

and the series expansion of E becomes

$$E = \sum_{p=0}^{\infty} D_p(e) (\tau - \tau_1)^p \tag{2}$$

Let $E = x + iy$ and $\tau = u + iv$ be the points of the E and τ complex planes, respectively. Equation (1) then is considered as an analytic function that maps the E plane on the τ plane conformally (angle preserving). The conformality is interrupted at the singular points of the function. Denoting

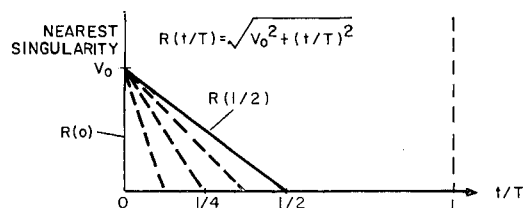


Fig. 2 The radius of convergence of one value of e